Binding Epitopes and Interaction Structure of the Neuroprotective Protease Inhibitor Cystatin C with β-Amyloid Revealed by Proteolytic Excision Mass Spectrometry and Molecular Docking Simulation

Paulina Juszczyk,[§,†,‡] Gabriela Paraschiv,[§,‡] Aneta Szymanska,[†] Aneta S. Kolodziejczyk,[†] Sylwia Rodziewicz-Motowidlo,[†] Zbigniew Grzonka,[†] and Michael Przybylski*[,§]

Laboratory of Analytical Chemistry and Biopolymer Structure Analysis, Department of Chemistry, University of Konstanz, 78457 Konstanz, Germany, and Department of Organic Chemistry, Faculty of Chemistry, University of Gdansk, 80-952 Gdansk, Poland

Received September 8, 2008

Human cystatin C (HCC) is a protease inhibitor with a propensity to form β-amyloid (Aβ)-like fibrils and to coassociate with amyloidogenic proteins. Recently, a specific interaction between HCC and Aβ has been found. Here, we report the identification of the Aβ and HCC binding epitopes in the Aβ−HCC complex, using a combination of selective proteolytic excision and high resolution mass spectrometry. Proteolytic excision of Aβ(1−40) on sepharose-immobilized HCC and MALDI-MS identified the epitope Aβ(17−28). On immobilized Aβ(1−40), affinity MS of HCC fragments identified a specific C-terminal epitope, HCC(101−117). Binding specificities of both epitopes were ascertained by ELISA and surface plasmon resonance and by direct electrospray MS of the HCC−Aβ epitope peptide complexes. A structure model of the HCC−Aβ complex by molecular docking simulation showed full agreement with the identified Aβ and HCC epitopes. Inhibition studies in vitro revealed Aβ-fibril inhibiting activity of the HCC(101−117)-epitope. The Aβ−HCC interacting epitopes provide lead structures of neuroprotective inhibitors for AD and HCC amyloidosis therapy.

Introduction

Alzheimer's disease (AD[a]) and AD-related neurodegenerative disorders have become the predominant form of progressive cognitive failure in elderly humans, a development presently accelerating because of the significant increase in life expectancy in the past decades. Consequently, uncovering details of AD pathology has become of paramount importance. Major neuropathological features in AD brain are cortical atrophy, neuronal loss, region-specific amyloid deposition, neuritic plaques, and neurofibrillary tangles.[1,2] A major constituent of amyloid fibrils in brains of patients with AD, as well as in aged individuals without any neurological disorder, is the β-amyloid polypeptide (Aβ). Aβ arises from a large precursor, the amyloid precursor protein (APP);[3,4] it is produced by normal cells and detected as a circulating peptide in plasma and cerebrospinal fluid (CSF) of healthy humans.[5,6] Although the physiological role of APP is not well understood, specific missense mutations confer autosomal dominant inheritance of AD (FAD) and have pointed out pathogenic, proteolytic processing mechanism(s).[6] The accumulation of Aβ, a 39−42 amino acid proteolytic fragment of APP, in neuritic AD plaques is thought to be causative for disease progression.[5,6] The N-terminal sequence of Aβ(1−42) is part of the extracellular region of APP, while the major C-terminal Aβ sequence is contained within the transmembrane domain.

Despite the lack of details on the mechanism(s) of formation of Aβ-derived plaques, studies toward the development of immunotherapeutic methods for AD have yielded therapeutically active antibodies capable of disaggregating Aβ-plaques. Both active immunization with preaggregated Aβ(1−42) and passive immunization with Aβ-specific antibodies have been shown to attenuate plaque deposition and neuritic dystrophy.[7−11] The epitope recognized by Aβ-plaque specific antibodies produced by immunization with Aβ has been identified by selective proteolytic excision (epitope excision) of the antigen−antibody complex in combination with high resolution mass spectrometry[12] to consist of a specific N-terminal sequence, Aβ(4−10).[12,13] In contrast, physiological Aβ-antibodies (Aβ-autoantiodies) have been recently identified in blood and CSF of healthy humans[14] and in intravenous IgG preparations (IVIgG); Aβ-autoantibodies specifically bind to human Aβ(1−40) and have been shown to inhibit Aβ-plaque deposition and neurotoxicity.[15−18] A specific carboxy-terminal Aβ-epitope has been identified to be targeted by Aβ-autoantibodies using epitope excision-mass spectrometry (M. Przybylski et al., *Abstracts of the 7th Australian Peptide Symposium*, Cairns, Australia, Oct 21−25, 2007; p 32), in contrast to Aβ-antibodies produced by active immunization.[17,18]

Although amyloid plaques in brains of AD patients contain Aβ-aggregates as a major consituent, immunohistochemical studies have shown the codeposition of several other proteins, such as the protease inhibitor cystatin C, apolipoprotein E, clusterin, transthyretin, and gelsolin.[19−22] In particular, the presence of human cystatin C (HCC) in amyloid deposits has found much interest[23,24] due to a wide spectrum of activities such as modulation of neuropeptide activation and neurite proliferation.[25,26] The 13 kDa protein HCC is a main cysteine protease inhibitor in mammalian body fluids[27,28] and occurs with high concentrations in CSF. While wild type cystatin C has no

* To whom correspondence should be addressed. Phone: (+49) 7531-883928. Fax: (+49) 7531-883097. E-mail: Michael.przybylski@uni-konstanz.de.

§ University of Konstanz.

† University of Gdansk.

‡ P.J. and G.P. contributed equally to this work.

[a] Abbreviations: AD, Alzheimer's disease; Aβ, β-amyloid peptide; HCC, human cystatin C; CAA, human cystatin C amyloidosis; APP, β-amyloid precursor protein; MS, mass spectrometry; MALDI, matrix-assisted laser desorption/ionization; FTICR, Fourier transform ion cyclotron resonence; ESI, electrospray ionization; TOF, time of flight; MD, molecular dynamics; SPR, surface plasmon resonance; HRP, horseradish peroxidase.

10.1021/jm801115e CCC: $40.75
Published on Web 03/24/2009

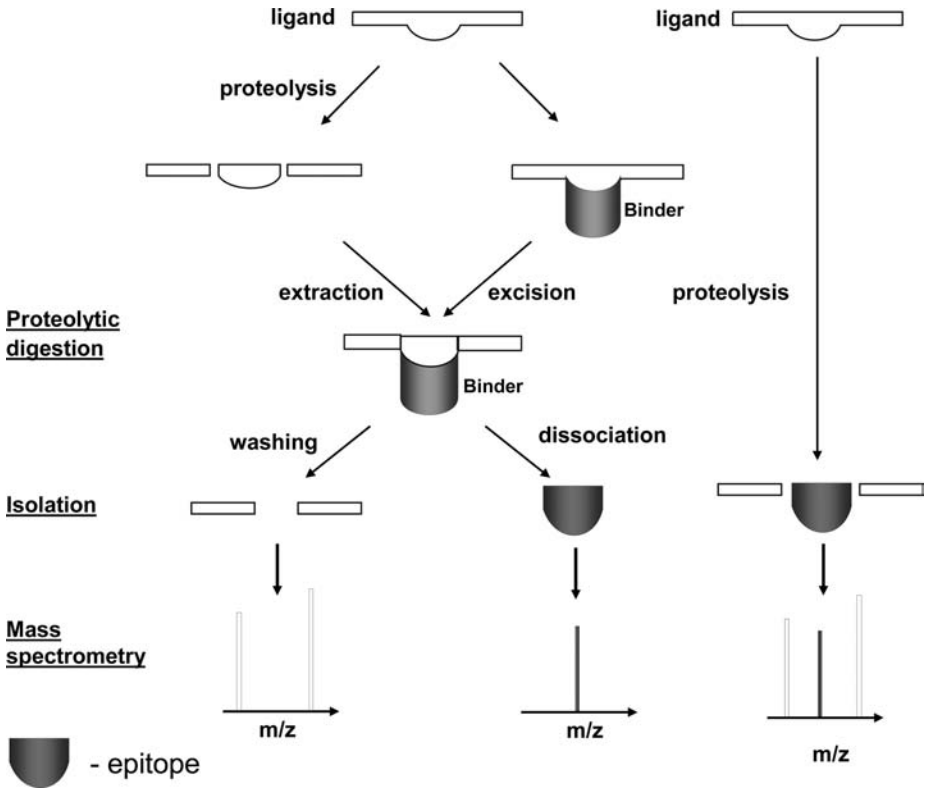

Figure 1. General analytical scheme of epitope identification analysis using the combination of proteolytic excision/extraction of a binder−ligand complex and mass spectrometry. In epitope excision the ligand (e.g., antigen) is bound to the immobilized binder (e.g., antibody) and the complex proteolytically degraded by proteases. In the epitope-extraction procedure the ligand is first degraded and the proteolytic mixture then applied to the immobilized binder. The affinity-bound peptide fragment(s) is subsequently eluted and analyzed by mass spectrometry.

aggregation tendency, the naturally occurring mutant L68Q shows a propensity to form amyloid fibrils and to cause hereditary cerebral hemorrhage of the amyloidosis-Icelandic type.[20−23] The presence of HCC in Aβ-plaques has been suggested to result from its binding to APP, or alternatively, HCC may bind to Aβ prior to the secretion or following the deposition in brain.[23] Sastre et al. found that association of HCC with Aβ causes an inhibition of fibril formation and suggested an N-terminal Aβ-epitope to be responsible for the interaction.[25]

The recent results suggesting an important role of HCC in the processing and/or aggregation of Aβ prompted our interest in the molecular characterization of the Aβ−HCC interaction. Here, we report the identification of the interacting epitopes of HCC and Aβ using proteolytic epitope excision mass spectrometry of the HCC−Aβ complex.[18] The general analytical scheme of the epitope excision-MS method is illustrated in Figure 1. The immobilized ligand−binder (antigen−antibody) complex is subjected to specific, limited proteolytic digestion followed by mass spectrometric analysis of the eluted affinity-bound epitope fragments. In the proteolytic step the epitope is protected from digestion because of the shielding of the ligand−binder interaction, enabling subsequent specific dissociation and MS analysis of the bound epitope(s).[18] In a variation of this approach ("epitope extraction") the ligand is first subjected to proteolytic digestion and the mixture of peptide fragments presented to the immobilized binder. By use of both approaches, the Aβ-epitope interacting with HCC was identified at a specific C-terminal sequence (Aβ(17−28)) interfering with the Aβ-aggregation; the analogous proteolytic-MS procedure with immobilized Aβ provided the identification of a specific Aβ-binding epitope at the C-terminus of HCC. Structures and affinities of both the Aβ and HCC epitopes were characterized by synthesis, ELISA, and surface plasmon resonance (SPR) binding studies and by direct mass spectrometric analysis of HCC−Aβ epitope peptide complexes. Furthermore, a structure model of the HCC−Aβ complex obtained by molecular docking simulation was in full agreement with the identified epitopes, and the synthetic HCC-epitope peptide showed Aβ-fibril inhibition effect in vitro.

Results

Identification of the Aβ-Epitope Recognized by Human Cystatin C. Both proteolytic excision mass spectrometry and extraction mass spectrometry were employed in the identification of the Aβ- and HCC-epitopes in the HCC−Aβ complex according to the general scheme (Figure 1), using a series of proteolytic enzymes. HCC was immobilized on NHS-activated Sepharose and the activity of the HCC affinity column ascertained by binding Aβ(1−40) and affinity mass spectrometry[17] which provided exclusively the Aβ molecular ion $(M + H)^+$ in the affinity−elution fraction (data not shown). Epitope excision-MS of the Aβ−HCC complex using Glu-C protease was performed by applying Aβ(1−40) onto the HCC column followed by digestion of the immune complex and extensive washing to remove noninteracting fragments (Figure 2). Digestion of free Aβ(1−40) in solution showed cleavage at all expected Glu residues (Glu-3, Glu-11, Glu-22) (Figure 2a). In contrast, the epitope elution fraction obtained upon acidification of the affinity-bound fragments provided only two carboxy-terminal Aβ-peptides; the Glu-22 peptide bond was found shielded from digestion indicating this residue to be part of the epitope (Figure 2, Table 1). The minimum Aβ-epitope sequence was identified by epitope excision-MS with pronase which cleaves free Aβ into the single amino acids. Epitope excision-MS using pronase provided a single Aβ-peptide in the affinity−elution fraction which was identified as Aβ(17−24),

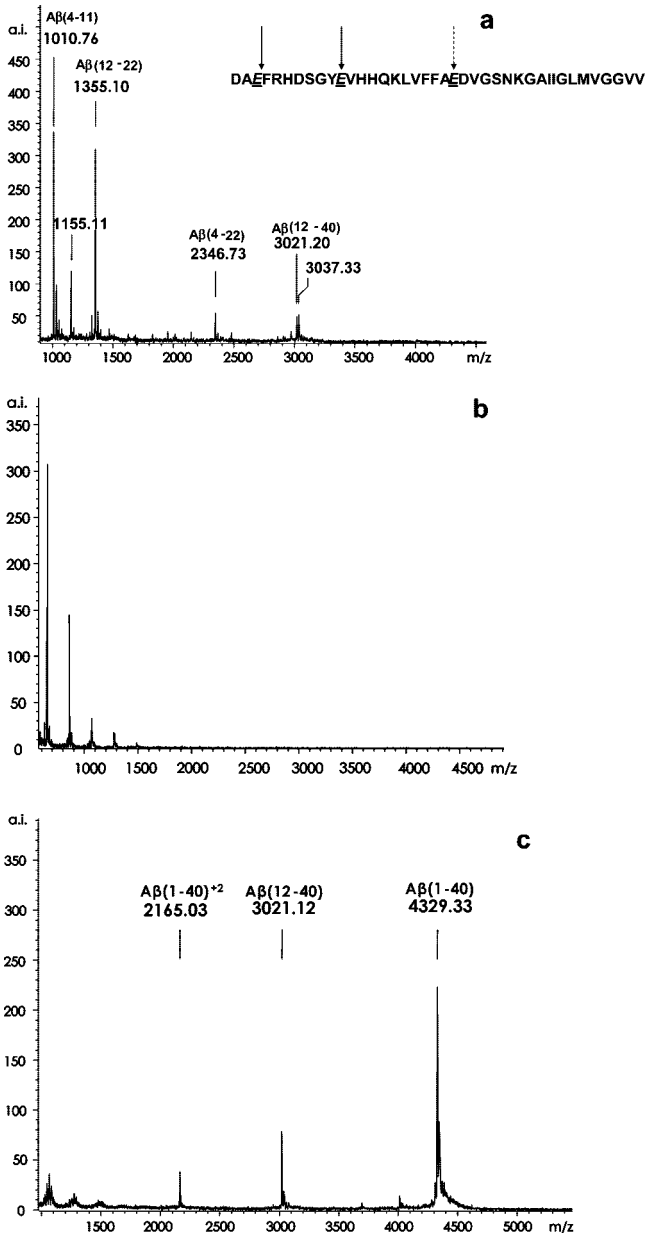

Figure 2. Mass spectrometric identification of the Aβ epitope binding to HCC: (a) MALDI-TOF-MS of the Glu-C protease digestion mixture of Aβ(1−40) in solution; (b) spectrum of the supernatant fraction after washing; (c) MALDI-MS of the elution fraction showing the epitope fragment Aβ(12−40) (M_r = 3022.12). Proteolytic cleavages yielding fragments identified upon epitope excision are indicated by solid arrows (E-3, E-11). The E-22 residue shielded from proteolytic digestion in the HCC−Aβ complex is indicated by a broken arrow.

LVFFAEDV (Figure 3). Corresponding epitope extraction- and excision-MS with different proteases (trypsin, Lys-C, carboxypeptidase Y) all provided the same epitope localization in the central to C-terminal domain of Aβ and ascertained that the N-terminal Aβ domain is not binding to HCC (see Table 1). Therefore, N-terminally truncated Aβ(12−40) subjected to epitope excision-MS at the same conditions provided the same minimal binding epitope, Aβ(17−24), while N-terminal Aβ-peptides did not show any binding to HCC.

ELISA binding studies with the synthetic Aβ peptides were in complete agreement with the mass spectrometric identification of the Aβ-epitope. While the synthetic Aβ(17−24) showed only minimal binding affinity, high affinity was found for Aβ(17−28), suggesting some conformational requirement for the Aβ-epitope binding to HCC. Because of these results, Aβ(17−28) was used as a model peptide for further affinity studies (see Figure 7).

Identification of the HCC-Epitope in the Aβ−HCC Complex. The analogous proteolytic excision-MS methodology was employed for identification of the HCC-epitope in the HCC−Aβ complex, using an Aβ(1−40) affinity column. Preliminary studies had shown that NHS-activated Sepharose is not suitable for immobilization of short peptides; furthermore, fragmentation was observed in proteolytic excision experiments with immobilized Aβ(1−40). However, a stable Aβ-affinity column was obtained by immobilization using an UltraLink-iodoacetyl matrix[13,17] to which the Aβ-peptide was linked by an additional N-terminal Cys residue and attached via thioether ligation. Prior to epitope excision-MS, tryptic digestion of HCC in solution was performed and analyzed by MALDI-MS which provided peptides fragments of nearly the complete sequence except for two small N- and C-terminal fragments (data not shown). Epitope-excision and -extraction-MS experiments were then performed with a series of proteases using conditions identical to those applied for the Aβ-epitope identification. MALDI-MS of the supernatant upon epitope excision with trypsin showed that the N-terminal part of HCC did not interact with Aβ; this domain is exchanged during 3D domain swapping and involved in dimer formation.[29] The elution fraction of the affinity-bound peptides provided only two C-terminal epitope peptides, HCC(93−120) and HCC(94−120); the Lys-114 residue was not cleaved in the complex and thus is shielded from digestion, indicating that the Aβ-binding site is located at the C-terminal domain of HCC (Figure 4a).

The identification of the exact epitope sequence was obtained by epitope excision-MS with pronase which provided identical results for intact HCC and the HCC(93−120) peptide (Figure 4b); furthermore, these results were fully confirmed by affinity studies with synthetic HCC(93−120) (Figures 5 and 6). In both cases the shortest proteolytic epitope eluted from the HCC−Aβ complex was identified as HCC(101−117). Affinity-MS and ELISA confirmed this peptide as the minimal Aβ-binding epitope of HCC.

Mass Spectrometric Characterization of the HCC−Aβ Epitope Peptide Complex. Further evidence for the specific interaction of the HCC- and Aβ-epitopes was obtained by direct high resolution ESI mass spectrometry of the complexes of HCC- and Aβ-peptides. The nano-ESI-FTICR mass spectrum of the peptide complex between the HCC(101−117) and the Aβ(17−28) epitopes is shown in Figure 5. The specific formation of a stoichiometric complex between the Aβ and HCC epitope peptides was ascertained by the triply and quadruply charged molecular ions $(M+3H)^{3+}$ (*m*/*z* 1070,1408) and $(M + 4H)^{4+}$ of the complex which were determined with a relative mass accuracy of approximately 5 ppm. Likewise, the complex between HCC(93−120) and Aβ(17−28) yielded molecular ions $(M + 3H)^{3+}$ (*m*/*z* 1497.6012) and $(M+4H)^{4+}$ (*m*/*z* 1123.4403) (Δm = 6.5 ppm; data not shown). Thus, the direct ESI-MS identification of the peptide complex ascertained the specific interaction of the C-terminal HCC epitope with the Aβ epitope located in the middle- to C- terminal domain.

Molecular Dynamics Simulation of the HCC−Aβ Complex. Molecular dynamics calculations were performed for sixteen HCC−Aβ complexes in which the initial structure of Aβ (α-helix or β-strand) was changed while the HCC structure was kept stable. After MD calculations the secondary structures of the Aβ peptides had changed in the regions of the interaction with HCC. In addition, we found that the initial structure of Aβ did not have a large influence on the structure and stability

Table 1. Aβ-Epitope Peptides Identified by Epitope-Excision MALDI-MS from Immobilized HCC with Different Proteases

protease	generated fragments	$M + H_{calc}$, *m/z*	$M + H_{found}$, *m/z*
trypsin	Aβ(6−40) HDSGYEVHHQKLVFFAEDVGSNKGAIIGLMVGGVV	3708.9	3709.5
chymotrypsin	Aβ(21−40) AEDVGSNKGAIIGLMVGGVV	1885.2	1886.5
	Aβ(17−28) LVFFAEDVGSNK	1325.5	1326.3
Glu-C	Aβ(12−40) VHHQKLVFFAEDVGSNKGAIIGLMVGGVV	3021.6	3021.1
Lys-C	Aβ(17−28) LVFFAEDVGSNK	1325.5	1326.2
carboxy-peptidase Y	Aβ(12−29) VHHQKLVFFAEDVGSNKG	2012.3	2012.5
pronase	Aβ(17−24) LVFFAEDV	938.4	938.6

of the HCC−Aβ complex (data not shown; see Figure 12 of the Supporting Information for a comparison). In most of the analyzed complexes, hydrophobic and electrostatic interactions between HCC and Aβ were formed. The stable HCC−Aβ complex (Figure 6) clearly shows hydrophobic interactions between Tyr-102, Val-104, and Trp-106 residues of HCC (colored in blue) and Phe-19, Phe-20, and Val-24 residues of Aβ (colored in red) forming a hydrophobic cluster. Moreover, in full agreement with the mass spectrometric epitope identifications, the carbonyl groups of Phe-19 and Asp-23 (βCO) of Aβ form stable hydrogen bonds with the Gln-107 (γNH) and Thr-109 (OH) residues of HCC. It may be suggested that the hydrophobic domains of Aβ and the L2 loop of HCC-protein "glue" together to form a stable complex. The L2 loop of HCC is covered by Aβ and not amenable to external interaction. The N- and C-terminal sequences of Aβ are not binding to HCC and therefore are amenable to cleavage by proteolytic enzymes.

Affinity Characterization of the Aβ- and HCC-Epitopes. The specificities and affinities of the epitope interactions were analyzed by ELISA of the HCC and Aβ peptides in a manner analogous to that employed for antibody binding to an antigen-coated plate. A suitable ELISA approach for the Aβ−HCC complex was developed to determine the affinities of Aβ peptides to HCC, by absorption of HCC on the ELISA plate and binding the N-terminally biotinylated Aβ-peptides via a spacer peptide (biotin-$(Gly)_5$-Aβ peptides), using an antibiotin detection antibody. No anti-HCC or anti-Aβ antibody was used to exclude a possible interference of the antibody epitope with the binding sites of the HCC−Aβ complex. Biotinylated peptide derivatives of full length Aβ(1−40), Aβ(12−40), Aβ(17−28), and Aβ(1−16) were tested in a comparative ELISA experiment (Figure 7a). All Aβ peptides comprising the HCC-binding epitope showed binding affinity to HCC, with Aβ(17−28) having the highest affinity, while the N-terminal peptide Aβ(1−16) did not show any binding. Thus, the ELISA results were in complete agreement with the mass spectrometric epitope identification.

Further comparative ELISA studies were performed with the Aβ(17−28) epitope using the C-terminal HCC peptides identified by epitope excision mass spectrometry, by coating the ELISA plate with intact HCC and the HCC(93−120), HCC(101−117), and HCC(101−114) fragments. The results confirmed the C-terminal HCC epitope, showing that the carboxy-terminal sequence is essential for binding affinity to Aβ (Figure 7b). In addition, studies using surface plasmon resonance (SPR) ascertained the C-terminal HCC epitope and provided the first quantitative affinity data for the Aβ- and HCC-interacting

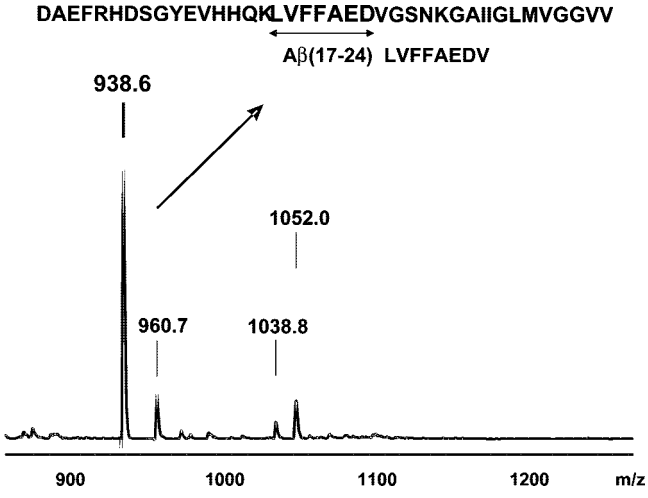

Figure 3. MALDI-MS of the elution fraction after epitope excision of Aβ(1−40) on immobilized HCC with pronase. The major product, Aβ(17−24), identified as the minimum epitope is indicated by an arrow. The epitope sequence, Aβ(17−25) (M_r = 1038), is present as a minor product.

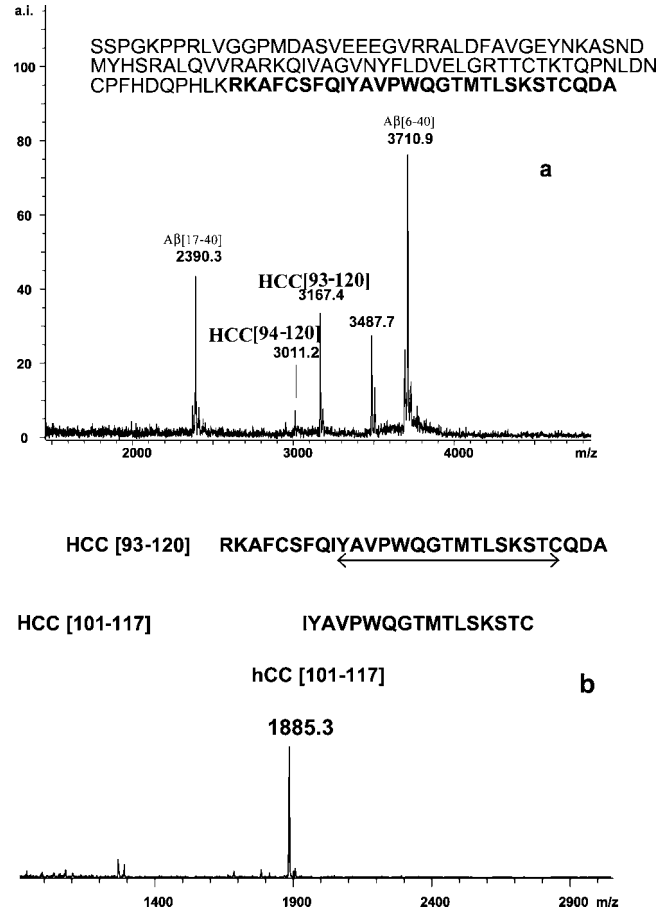

Figure 4. Mass spectrometric identification of the HCC binding epitope to Aβ(1−40). (a) Tryptic HCC fragments eluted after epitope excision from the Aβ(1−40)−HCC complex showing two peptide fragments, HCC (93−120) and HCC (94−120) (MW 3167.4 and 3011.2). Bold residues in the HCC sequence indicate the minimum epitope, HCC-(101−117) (IYAVPWQGTMTLSKSTC). (b) MALDI-MS of the elution fraction showing identification of the HCC epitope, HCC(101−117), upon epitope excision from immobilized Aβ(1−40) using pronase.

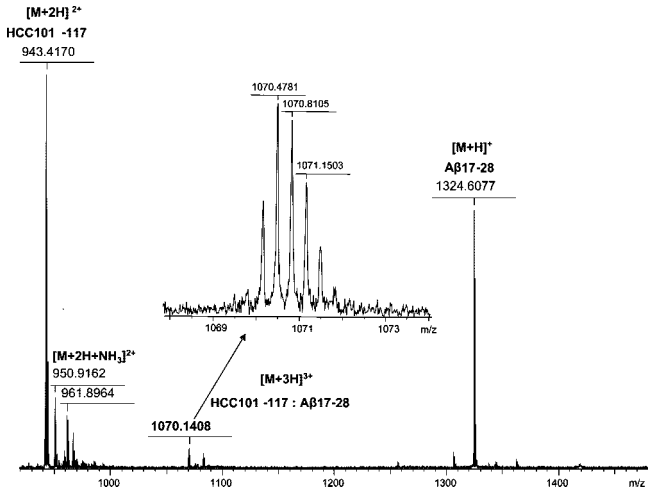

Figure 5. Nano-ESI-FTICR mass spectrum of the pepide complex of HCC(101−117) with Aβ(17−28).

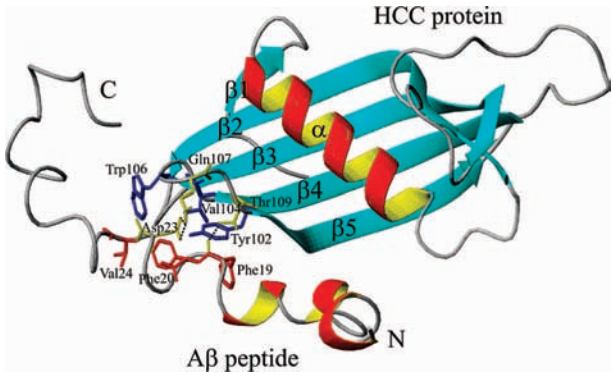

Figure 6. Interaction structure of the HCC−Aβ complex revealed by molecular dynamics simulation. Hydrophobic interactions between HCC and Aβ, Tyr-102, Val-104, and Trp-106 residues of HCC are colored in blue; Phe-19, Phe-20, Val-24 residues of Aβ are colored in red. Hydrogen bonds between Gln-107 and Thr-109 residues of HCC and Asp-23 and Phe-19 of Aβ are indicated by black dashed lines, respectively; amino acids and carbonyl groups (Phe-19) forming hydrogen bonds are colored in yellow.

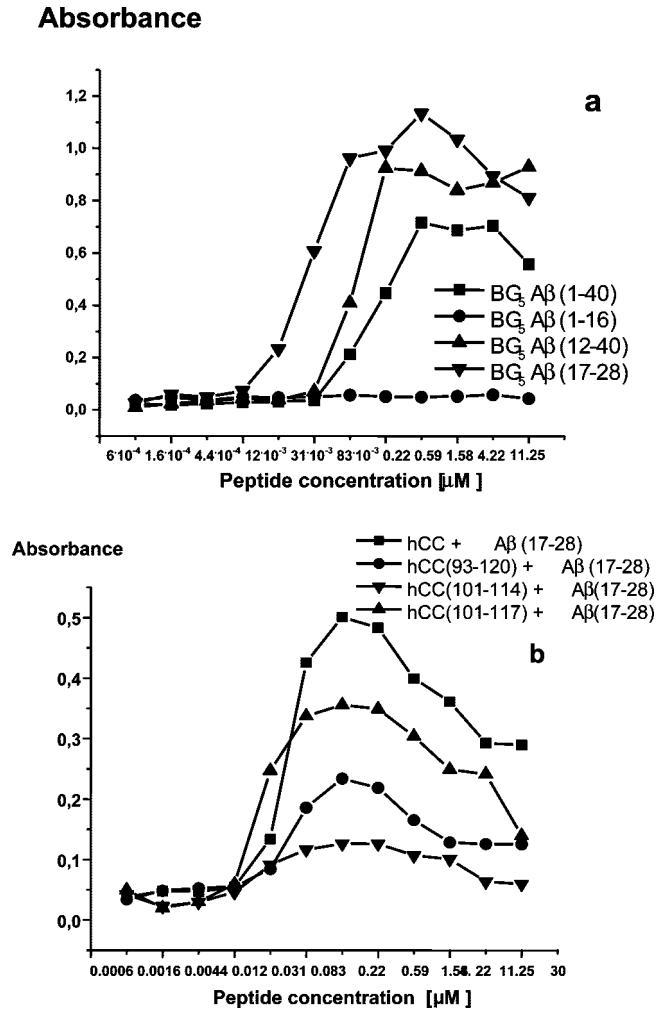

Figure 7. (a) Binding of Aβ peptides to HCC. The ELISA plate was coated with HCC and incubated with biotinylated Aβ peptides followed by incubation with antibiotin HRP as described in the Experimental Section. (b) Direct ELISA of the binding of HCC epitope peptides to Aβ. The plate was coated with HCC and HCC fragment, and after complex formation with biotin-$(Gly)_5$-Aβ(17−28) the plate was incubated with antibiotin HRP.

epitopes. The initial SPR determinations of the HCC(93−120) and HCC(101−117) peptides bound to biotin-$(Gly)_5$-Aβ(1−40) on a gold-coated streptavidin biosensor chip provided K_D values of 3.9 and 7.5 μM, respectively, while intact HCC yielded a K_D of approximately 2.5 μM. Detailed SPR analyses of the minimum Aβ- and HCC-epitopes are presently carried out, together with structural studies of the peptide−peptide complexes.

Inhibition of Aβ-Fibril Formation by C-Terminal HCC Epitopes. Inhibition studies of Aβ-oligomerization and fibril formation were performed with intact HCC in comparison with the C-terminal HCC epitope as shown in Table 2, using an in vitro assay of Aβ-oligomerization.[25] For formation of Aβ-oligomers, Aβ(1−40) was first dissolved in 100% TFE to ensure reformation of monomers, and the sample was then lyophilized and redissolved in DMSO to obtain stable monomer solutions. The samples were then diluted to a final peptide concentration of 10 μM in 50 mM phosphate buffer, pH 7.4, and a 10% final DMSO, and Aβ(1−40) with and without HCC-epitope peptides were incubated at 37 °C for up to 72 h. Prior to analysis by SDS−PAGE, the samples were centrifuged at 13000*g* for 5 min and then lyophilized. Fibril inhibition was determined as the relative decrease of oligomer bands, using the software QuantityOne (see example in Figure 9 of Supporting Information).

Table 2. Relative Inhibition (Inhibition of Oligomer Bands) of Aβ-Fibril Formation by HCC-Epitope Peptides after 72 h

HCC-peptide/Aβ-peptide	HCC-epitope (μM)	% fibril inhibition
HCC(93−120)/Aβ(1−40)	10	5
HCC(93−120)/Aβ(1−40)	100	35
HCC(101−117)/Aβ(1−40)	10	12
HCC(101−117)/Aβ(1−40)	100	51

These initial comparative quantifications clearly showed a time- and concentration-dependent inhibitory effect of the HCC epitope peptides on the formation of Aβ-oligomer aggregates, with the highest relative effect obtained for the HCC (101−117)-peptide (Table 2). Detailed quantitative determinations of in vitro fibril inhibition by the HCC-epitope peptides, using electrophoretic and microscopic methods, are carried out at present.

Discussion

Although the colocalization of cystatin C and Aβ has been demonstrated in cerebral arteries of CAA patients,[24] in cerebral vasculature and brain parenchyma of AD patients,[28] and in muscle cells of patients with age-dependent inclusion body myositis,[25] the biological role of the interaction and mechanism

of the HCC−Aβ coaggregation has been hitherto unknown. In this study we investigated the binding epitopes between HCC and Aβ using a molecular affinity mass spectrometry approach[17] and present the first identification of the epitope sequences and interaction structure of the Aβ−HCC complex.

The results of proteolytic excision mass spectrometry show that the HCC binding site is located in the central region of Aβ within residues (17−28) which is critically important for the Aβ structure and aggregation. The Aβ-epitope comprises a part of the hydrophobic core at residues (17−22) (LVFFA) and the β-turn for fibril formation located within residues (25−28).[30] Tycko et al. reported the residues (12−24) and (30−40) to be involved in the formation of the parallel β-sheet structure in fibrils.[31,32] The residues (25−35) are part of the highly hydrophobic C-terminal region of Aβ which is crucial for oligomerization and fibril formation, [33] while residues (17−21) have been proposed to be involved in side chain interactions and the dimerization of Aβ.[30] Furthermore, it been suggested that the sequence KLVFFAE (16−22) has an inhibitory effect on fibril formation, indicating the importance of these residues for Aβ assembly.[32,34] This region is very sensitive to single site mutations which cause significant changes of structure, aggregation, and toxicity of Aβ.[34−36] The HCC binding results confirm that HCC efficiently binds to this region and by blocking the residues (17−28) might influence Aβ oligomerization, plaque formation, and neurotoxicity. The HCC binding site in Aβ identified here is different from that proposed by Sastre et al.,[25] since our results ascertain binding at the central domain of Aβ, not at an N-terminal sequence. Thus, the previously observed blocking of HCC binding to Aβ by an anti-Aβ(1−17) antibody may be well explained by steric hindrance of the protein at the binding site starting at Leu-17. Selenica et al. showed that HCC reduced the in vitro formation of soluble Aβ-oligomers and protofibrils; however, HCC did not dissolve preformed Aβ-oligomers.[23] The present results indicate that HCC is interacting with monomeric Aβ, and binding of the protein to the central domain of Aβ may effectively suppress aggregation by blocking the access to the hydrophobic C-terminal part of Aβ, thus inhibiting interaction with a second Aβ molecule. In preformed oligomers the hydrophobic core is involved in Aβ--Aβ interactions, thus preventing the access of HCC. This result is in agreement with the hypothesis that the presence of HCC in Aβ solution can decrease oligomerization[25] and slow down the aggregation process.

The HCC binding site in Aβ identified is localized in a similar position to the Aβ-epitope recognized by physiological Aβ-autoantibodies which seem to play a neuroprotective role in the oligomerization of Aβ.[16] Thus, a neuroprotective effect might be suggested for the binding of HCC binding to Aβ. The Aβ-binding site identified in HCC at residues (101−117) is located in the C-terminal part within the L2 loop and β5 strand of HCC which comprise the external part of the protein and are exposed to the environment.[27] The C-terminal epitope enables interaction of Aβ with the L2-β5 part without any restriction. The identification of the binding epitope in HCC may be of interest for comparative oligomerization and fibrillation studies of HCC and its amyloidogenic mutant L68Q which has a similar structure to HCC;[20,25] however, it remains to be determined if this mutant has a similar Aβ binding epitope. The knowledge of the binding epitope may be of interest for future studies of HCC fibril formation, since fibrils can be easily formed with the L68Q HCC mutant by 3D domain swapping. In a model postulated by Jaskolski[29] the Aβ binding site is located in the center of the fibrils which might enable the opportunity to block the interaction between cystatin molecules by binding of Aβ to the C-terminal part of HCC.

Conclusions

The interaction of HCC with Aβ may be an important mechanism related to neurotoxicity and oligomerization of Aβ and might play a regulating role in Aβ amyloidogenesis. The identification of the binding epitope of HCC in the central domain of Aβ confirmed the importance of this protease inhibitor for the aggregation process and amyloidogenesis, since blocking the hydrophobic core may inhibit Aβ oligomerization and regulate fibril production. On the other hand, the identification of the binding site in HCC should be of importance for oligomerization studies of cystatin C, and new oligomerization inhibitors may be designed on the basis of the HCC-epitope.[37,38]

Experimental Section

Synthesis of Aβ and HCC Peptides. Aβ and HCC peptides were synthesized by solid phase peptide synthesis (SPPS) with a semiautomated peptide synthesizer EPS-221 (Intavis, Langenfeld, Germany), using general conditions of synthesis and purification as previously described.[13] All syntheses were performed on a NovaSyn TGR resin (0.23 mmol/g coupling capacity), using 9-fluorenylmethoxycarbonyl/*tert*-butyl (Fmoc/*t*Bu) chemistry with the following side chain protected amino acid derivatives: Fmoc-Asp(O*t*Bu)-OH, Fmoc-Ala-OH, Fmoc-Glu(O*t*Bu)-OH, Fmoc-Phe-OH, Fmoc-Arg(Pbf)-OH, Fmoc-His(Trt)-OH, Fmoc-Ser(*t*Bu)-OH, Fmoc-Gly-OH, Fmoc-Tyr(*t*Bu)-OH, Fmoc-Val-OH, Fmoc-Gln(Trt)-OH, Fmoc-Lys(Boc)-OH, Fmoc-Leu-OH, Fmoc-Asn(Trt)-OH, Fmoc-Ile-OH, Fmoc-Met-OH. As an example, the synthesis of *N*-biotin-$(Gly)_5$-Aβ(1−40) was performed with the following synthetic protocol: (i) DMF washing (3 × 1 min); (ii) Fmoc deprotection for 15 min using 2% DBU and 2% piperidine in DMF; (iii) DMF washing (6 × 1 min); (iv) coupling of 5 equiv of Fmoc amino acid/PyBOP/NMM in DMF for 45 min; (v) DMF washing (3 × 1 min). After completion of the synthesis, the N-terminus was biotinylated using 5 equiv of D-(+)-biotin/PyBOP/NMM. The peptides were then cleaved from the resin at 25 °C for 3 h using a mixture of TFA, triethylsilane, and deionized water (95:2.5:2.5, v/v/v). The crude products were precipitated with cold *tert*-butyl methyl ether, washed three times with diethyl ether, and solubilized in 5% aqueous acetic acid prior to freeze-drying.

The crude peptides were purified by semipreparative HPLC on a Vydac C4 column, with 80% acetonitrile in aqueous 0.1% trifluoroacetic acid (TFA, solvent B) and with 0.1% TFA in MilliQ water (solvent A) as mobile phases. Specific elution conditions were evaluated for each peptide, depending on relative hydrophobicities and solubilities of the Aβ peptides. All peptides were analyzed by MALDI-TOF-MS and MALDI-FTICR-MS, yielding the expected protonated average-isotope (MALDI-TOF) and monoisotopic (MALDI-FTICR) molecular ions. Relative purities of Aβ- and HCC-peptides were assessed by HPLC and were higher than 92%. Details of analytical data, HPLC, and mass spectra of all synthetic peptides are shown in Table 1 and Figures 1−8 of the Supporting Information.

Expression and Purification of Cystatin C. Plasmid pHD313 was obtained as a kind gift from Prof. Anders Grubb (University Hospital, Lund, Sweden), carrying the human cystatin C gene as a fusion protein with OmpA signal peptide for periplasmic expression. The protein was overexpressed in *E.coli* strain C41(DE3) as described previously. The harvested bacteria were resuspended in 10 mM Tris, pH 7.4, containing 10% glycerol (10 mL/1 L of culture) and then twice flash-frozen and thawed, leading to partial breakage of the bacterial outer membrane and release of proteins from the periplasmic space.[39] The sample was then centrifuged and the clear supernatant applied onto an S-Sepharose column equilibrated in 10 mM Tris-buffer containing 5% glycerol, pH 7.4 (buffer A). Adsorbed proteins were

eluted with an increasing salt gradient comprising 10 mM Tris, 1 M NaCl, and 5% glycerol, pH 7.4 (buffer B). The HCC fractions were collected, dialyzed extensively against 10 mM ammonium bicarbonate (pH 8), and lyophilized. The protein purity was characterized by SDS−PAGE and UV spectroscopy.

Sepharose Immobilization of HCC. A sample of approximately 100 μg of HCC was dissolved in 0.2 mL of coupling buffer containing 0.2 M $NaHCO_3$ and 0.5 M NaCl (pH 8.3), and the solution was added to 0.06 mg of dry NHS-activated Sepharose. The coupling reaction was carried out for 1 h at 25 °C under vigorous shaking, and the reaction mixture was loaded onto a 1 mL microcolumn (MoBiTec, Goettingen, Germany) and washed sequentially with blocking solution (0.1 M aminoethanol, 0.5 M NaCl, pH 8.3) and washing solution (0.2 M CH_3COONa, 0.5 M NaCl, pH 4.0). The column was incubated for 1 h at 25 °C with blocking solution followed by a second washing step as described above. In the final step the column was washed with 10 mL of 5 mM Na_2HPO_4, 150 mM NaCl, pH 7.5, and then stored at 4 °C.

Immobilization of Aβ(1−40). A solution of 2 mL of UltraLink iodoacetyl gel slurry (Pierce, Germany) containing approximately 1 mL of gel was placed in a microcolumn (MoBiTec, Goettingen, Germany). The gel was washed 5 times with coupling buffer (50 mM Tris, 5 mM EDTA, pH 8.5), and 469.8 μg of Cys-Aβ(1−40) was added and mixed with the gel for 15 min at 25 °C. The column was incubated for 30 min without mixing and, after draining off the liquid, washed three times with coupling buffer and then blocked with L-cysteine (50 mM L-Cys in coupling buffer; 15 min mixing and 30 min incubation without mixing). Finally, the column was washed 3 times with 1 M NaCl and 5 times with storage buffer (100 mM PBS, 150 mM NaCl, pH 7.2) and stored at 4 °C.

Affinity Isolation of Aβ(1−40) on HCC-Sepharose. HPLC-purified Aβ(1−40) (10 μg) was added onto the HCC-Sepharose column equilibrated in PBS (pH 7.5) and incubated for 2 h at 25 °C. Unbound material was removed by washing with 50 mL of PBS. The remaining affinity-bound HCC−Aβ complex was dissociated with 2 × 500 μL of 0.1% aqueous TFA; isolated Aβ-peptide was analyzed by MALDI-MS.

Epitope-Excision and -Extraction Mass Spectrometry. For proteolytic epitope excision mass spectrometry, the Aβ-complex on immobilized HCC was prepared and excess unbound Aβ(1−40) removed by washing as described above. The Aβ−HCC complex was then digested for 2 h with 1 μg of trypsin at 27 °C and in the same manner with chymotrypsin for 2 h at 25 °C and with pronase for 1 h at 40 °C. The supernatant fractions containing unbound digestion products were removed by washing with 20 mL of PBS. The remaining affinity-bound peptides were dissociated by addition of 500 μL of 0.1% aqueous TFA (pH 2.5) and fractions collected in Eppendorf cups and lyophilized until mass spectrometric analysis.

For epitope extraction mass spectrometry, proteolytic digestion of Aβ(1−40) was performed with the same proteases at identical conditions as described above, and the reaction mixtures were applied onto the HCC-Sepharose affinity column. The digestion mixtures were equilibrated with the column for 2 h at 25 °C, the supernatants containing unbound peptide fragments removed by washing, and the epitope fractions recovered by elution with 0.1% TFA as described above.

Epitope-Excision Mass Spectrometry of HCC on Immobilized Aβ(1−40). Epitope identification of HCC using both epitope-excision and -extraction mass spectrometry was performed using identical reaction conditions as described above for the Aβ-epitope analysis, after binding of HCC on the Aβ-UltraLink iodoacetyl affinity column. HCC (30 μg) was applied onto the Aβ-affinity column for each digestion experiment, and washing and elution steps were performed in an identical manner as described above.

ELISA and SPR Affinity Studies. ELISA studies of HCC with Aβ peptides were performed by applying 100 μL of HCC (1 μM) on a 96-well microtiter plate. After blocking unspecific binding sites with 5% BSA in PBS/0.1% Tween, the plate was coated with serial dilutions of N-biotinylated Aβ-peptides (*N*-biotinyl-$(Gly)_5$-Aβ). The HRP-conjugated detection antibody (antibiotin−HRP) was allowed to interact for 1 h with the monoclonal antibiotin−HRP antibody, and wells were washed three times with PBS solution and subsequently with 50 mM sodium phosphate−citrate buffer, pH 5.0. Binding affinities were determined by addition of 100 μL/well 0.1% *o*-phenylenediamine dihydrochloride (OPD) in phosphate−citrate buffer containing 0.006% H_2O_2 and absorbance measured at 450 nm with a Wallac 1420 Victor ELISA plate counter (Perkin-Elmer, Überlingen, Germany).

Affinity studies between HCC(93−120) and biotin-G_5-Aβ(1−40) were performed with a Biacore T100 instrument (Biacore SA, Uppsala, Sweden). The experiments were done on a sensor chip SA designed for biotinylated peptides. SPR measurements resulting from unspecific binding were done for both reference and sample channels; after substraction of the signal from the reference channel, a K_D of 3.9 μM was obtained.

Inhibition Assay of Aβ-Oligomerization by HCC Peptides. The gels were prepared using the minigel instrument MiniProtean from BioRad. Samples were dissolved in 50 μL of running buffer (25% glycerol, 4% SDS, Coomassie) and added to the 12% gel (8.4 mL MilliQ, 6 mL of 4× separation buffer, 9.6 mL of acrylamide solution, 125 μL of APS, 20 μL of TEMED). The power/PAC 1000 instrument from Bio-Rad at constant current was used for gel electrophoresis in two steps: (a) 60 V when samples were in the stacking gel; (b) 120 V when samples were in the separating gel.

Mass Spectrometry. MALDI-TOF-MS analyses were carried out on a Bruker (Bruker Daltonics, Germany) Biflex ITM linear TOF mass spectrometer equipped with a nitrogen UV laser (λ = 337 nm) and a dual channel plate detector, at conditions as previously described.[17] Samples were dissolved in 0.1% trifluoroacetic acid and desalted using the Zip-Tip procedure. High resolution FTICR mass spectrometry was performed with a Bruker (Bruker Daltonics, Bremen, Germany) APEX II FTICR instrument equipped with an actively shielded 7 T superconducting magnet, a cylindrical infinity ICR analyzer cell, and an external Bruker Apollo-II nanoelectrospray ion source.[40] Sample preparation of HCC−Aβ epitope complexes was carried out with 10 μL aliquots of freshly prepared solutions of Aβ(17−28) (100 μM; M_r = 1323.68) in deionized water, which were added to 10 μL of an equimolar solution of HCC(101−117) or HCC(93−120) in 0.5 mM ammonium acetate, pH 6. After incubation of the HCC−Aβ peptide complex for 3 h at 25 °C, the solution was infused in the Apollo-II electrospray ionization source at a flow rate of 4 μL/min. FTICR mass spectra were obtained by accumulation of 32 single scans, with the capillary exit voltage set to 50 V for ion desolvation external accumulation of ions in a radiofrequency-only hexapole for 0.05 s before transfer into the ICR cell. The capillary voltage was adjusted between 960 and 1120 V until a stable spray was obtained. Other experimental conditions were as follows: setting of skimmer 1, 15; setting of skimmer 2, 7; rf amplitude, 600; ionization pulse time, 2 ms; mass resolution, approximately 150 000. Acquisition of spectra was carried out with the Bruker Daltonics software XMASS and the corresponding programs for mass calculation, data calibration, and processing.

Molecular Dynamics Calculations. For molecular dynamics calculations, an initial complex HCC−Aβ peptide ligand was built from the HCC monomer[20] and full length Aβ(1−40), or the Aβ(17−42) fragment. Starting conformations employed for Aβ were either helical (PDB code 1Z0Q, Aβ(1−40)) or β-hairpin (PDB code 2BGE, Aβ(17−42)). Approximately 30 000 HCC−Aβ starting complexes were built using ClusPro[41] and GRAMM-X[42] programs. For subsequent molecular dynamics calculations, only those complexes were selected in which the Aβ(17−28) fragment interacted with the (101−117) fragment of the HCC protein. In the selection procedure seven complexes of HCC with α-helical Aβ and nine complexes with β-hairpin Aβ were obtained (see Supporting Information Figure 11). The differences between the 16 complexes were mainly related to the side chain arrangements or to the arrangements of N- and C-terminal ends of Aβ and HCC ($N^{A\beta}$- to N^{HCC}- or $N^{A\beta}$- to C^{HCC}-terminus). Simulations were carried out using the AMBER 8.0 program (University of California, San

Francisco) and the all-atom parm94 force field. The crude complexes were initially minimized in vacuo to remove close van der Waals contacts. Before surrounding the HCC−ligand complex with water molecules, Na^+ and Cl^- charge balancing counterions were added in positions with favorable ionic interactions to neutralize charges on the HCC−ligand surface, and all structures were optimized by energy minimization in water. After minimization, the molecular dynamics for all complexes were calculated. Simulations of complexes in solution were performed under periodic boundary conditions in a closed, isothermal, isobaric (NTP) ensemble. Throughout, the simulation solute and solvent were coupled to a constant-temperature (300 K) heat bath and a constant-pressure ($P = 1$ atm) bath. All hydrogen-containing bonds were constrained using the SHAKE algorithm allowing a time step of 0.001 ps. An Ewald summation was used for nonbonded interactions, and coordinates were saved every 1000 steps. The time during all molecular dynamics simulations was 3000 ps. The time period of MD was about 3000 ps without constraints. Four of the 16 complexes (complexes **5**, **7**, **8**, and **11** in Figure 11 of Supporting Information) started to dissociate during MD time; therefore, for these complexes the MD calculations were interrupted. Refinement analysis was carried out using the carnal program from the AMBER package and MolMol graphical program.[43] Hydrogen bonds were assumed stable when their occurrence was more than 50% in MD time. In six of 12 complexes, three stable intermolecular hydrogen bonds were found. Hydrophobic interactions were evaluated by visual estimation of the hydrophobic interactions in the final HCC−Aβ complex structures (see Figure 13 of the Supporting Information for an example).

Acknowledgment. We gratefully acknowledge the expert assistance of Dr. Marilena Manea and Reinhold Weber in high resolution mass spectrometry and affinity MS procedures. This work has been supported the EU (EU network "Human Proteome Binders"), the University of Konstanz, Germany, and by grant No. 4233/H03/2007/32, University of Gdansk, Poland.

Supporting Information Available: HPLC, purities, and mass spectra of the synthetic HCC and Aβ peptides; example of SDS−PAGE of the Aβ-fibril inhibition by HCC epitope peptides at 72 h; HCC−Aβ complex structures and details of molecular dynamics calculations in the molecular docking procedures. This material is available free of charge via the Internet at http://pubs.acs.org.

References

(1) Glenner, G. G.; Wong, C. W. Alzheimer's disease and Down's syndrome: sharing of a unique cerebrovascular amyloid fibril protein. *Biochem. Biophys. Res. Commun.* **1984**, *122*, 1131–1135.
(2) Hardy, J.; Selkoe, D. J. The amyloid hypothesis of Alzheimer's disease: progress and problems on the road to therapeutics. *Science* **2002**, *297*, 353–356.
(3) Kang, J.; Lemaire, H. G.; Unterbeck, A.; Salbaum, J. M.; Masters, C. L. The precursor of Alzheimer's disease amyloid A4 protein resembles a cell-surface receptor. *Nature* **1987**, *325*, 733–736.
(4) Tanzi, R. E.; Gusella, J. F.; Watkins, P. C.; Bruns, G. A.; St George-Hyslop, P. Amyloid beta protein gene: cDNA, mRNA distribution, and genetic linkage near the Alzheimer locus. *Science* **1987**, *235*, 880–884.
(5) Calero, M.; Rostagno, A.; Frangione, B.; Ghiso, J. Clusterin and Alzheimer's disease. *Subcell. Biochem.* **2005**, *38*, 273–298.
(6) Anderson, D. H.; Talaga, K. C.; Rivest, A. J.; Barron, E.; Hageman, G. S. Characterization of beta amyloid assemblies in drusen: the deposits associated with aging and age-related macular degeneration. *Exp. Eye Res.* **2004**, *78*, 243–256.
(7) Bard, F.; Cannon, C.; Barbour, R.; Burke, R. L.; Games, D. Peripherally administered antibodies against amyloid beta-peptide enter the central nervous system and reduce pathology in a mouse model of Alzheimer disease. *Nat. Med.* **2000**, *6*, 916–919.
(8) Schenk, D.; Barbour, R.; Dunn, W.; Gordon, G.; Grajeda, H. Immunization with amyloid-beta attenuates Alzheimer-disease-like pathology in the PDAPP mouse. *Nature* **1999**, *400*, 173–177.
(9) DeMattos, R. B.; Bales, K. R.; Cummins, D. J.; Dodart, J. C.; Paul, S. M. Peripheral anti-A beta antibody alters CNS and plasma A beta clearance and decreases brain A beta burden in a mouse model of Alzheimer's disease. *Proc. Natl. Acad. Sci. U.S.A.* **2001**, *98*, 8850–8855.
(10) Janus, C.; Pearson, J.; McLaurin, J.; Mathews, P. M.; Jiang, Y. A beta peptide immunization reduces behavioural impairment and plaques in a model of Alzheimer's disease. *Nature* **2000**, *408*, 979–982.
(11) Hock, C.; Konietzko, U.; Streffer, J. R.; Tracy, J.; Signorell, A. Antibodies against beta-amyloid slow cognitive decline in Alzheimer's disease. *Neuron* **2003**, *38*, 547–554.
(12) McLaurin, J.; Cecal, R.; Kierstead, M. E.; Tian, X.; Phinney, A. L. Therapeutically effective antibodies against amyloid-beta peptide target amyloid-beta residues 4−10 and inhibit cytotoxicity and fibrillogenesis. *Nat. Med.* **2002**, *8*, 1263–1269.
(13) Tian, X.; Cecal, R.; McLaurin, J.; Manea, M.; Stefanescu, R. Identification and structural characterisation of carboxy-terminal polypeptides and antibody epitopes of Alzheimer's amyloid precursor protein using high-resolution mass spectrometry. *Eur. J. Mass Spectrom. (Chichester, Engl.)* **2005**, *11*, 547–556.
(14) Du, Y.; Dodel, R.; Hampel, H.; Buerger, K.; Lin, S. Reduced levels of amyloid beta-peptide antibody in Alzheimer disease. *Neurology* **2001**, *57*, 801–805.
(15) Du, Y.; Wei, X.; Dodel, R.; Sommer, N.; Hampel, H. Human anti-beta-amyloid antibodies block beta-amyloid fibril formation and prevent beta-amyloid-induced neurotoxicity. *Brain* **2003**, *126*, 1935–1939.
(16) Dodel, R. C.; Du, Y.; Depboylu, C.; Hampel, H.; Frolich, L. Intravenous immunoglobulins containing antibodies against beta-amyloid for the treatment of Alzheimer's disease. *J. Neurol. Neurosurg. Psychiatry* **2004**, *75*, 1472–1474.
(17) Stefanescu, R.; Iacob, R. E.; Damoc, E. N.; Marquardt, A.; Amstalden, E. Mass spectrometric approaches for elucidation of antigen−antibody recognition structures in molecular immunology. *Eur. J. Mass Spectrom. (Chichester, Engl.)* **2007**, *13*, 69–75.
(18) Przybylski, M.; Stefanescu, R.; Manea, M.,; Bacher, M.; Dodel, R. Diagnosis and Treatment of Alzheimer's and Other Neurodementing Diseases. PCT Patent Appl. WO 2008/084402A2, July 17, 2008; University of Konstanz, University of Marburg.
(19) Levy, E.; Sastre, M.; Kumar, A.; Gallo, G.; Piccardo, P. Codeposition of cystatin C with amyloid-beta protein in the brain of Alzheimer disease patients. *J. Neuropathol. Exp. Neurol.* **2001**, *60*, 94–104.
(20) Rodziewicz-Motowidlo, S.; Wahlbom, M.; Wang, X.; Lagiewka, J.; Janowski, R. Checking the conformational stability of cystatin C and its L68Q variant by molecular dynamics studies: why is the L68Q variant amyloidogenic? *J. Struct. Biol.* **2006**, *154*, 68–78.
(21) Calero, M.; Pawlik, M.; Soto, C.; Castano, E. M.; Sigurdsson, E. M. Distinct properties of wild-type and the amyloidogenic human cystatin C variant of hereditary cerebral hemorrhage with amyloidosis, Icelandic type. *J. Neurochem.* **2001**, *77*, 628–637.
(22) Levy, E.; Jaskolski, M.; Grubb, A. The role of cystatin C in cerebral amyloid angiopathy and stroke: cell biology and animal models. *Brain Pathol.* **2006**, *16*, 60–70.
(23) Selenica, M. L.; Wang, X.; Ostergaard-Pedersen, L.; Westlind-Danielsson, A.; Grubb, A. Cystatin C reduces the in vitro formation of soluble Abeta1−42 oligomers and protofibrils. *Scand. J. Clin. Lab. Invest.* **2007**, *67*, 179–190.
(24) Vattemi, G.; Engel, W. K.; McFerrin, J.; Askanas, V. Cystatin C colocalizes with amyloid-beta and coimmunoprecipitates with amyloid-beta precursor protein in sporadic inclusion-body myositis muscles. *J. Neurochem.* **2003**, *85*, 1539–1546.
(25) Sastre, M.; Calero, M.; Pawlik, M.; Mathews, P. M.; Kumar, A. Binding of cystatin C to Alzheimer's amyloid beta inhibits in vitro amyloid fibril formation. *Neurobiol. Aging* **2004**, *25*, 1033–1043.
(26) Carrette, O.; Demalte, I.; Scherl, A.; Yalkinoglu, O.; Corthals, G. A panel of cerebrospinal fluid potential biomarkers for the diagnosis of Alzheimer's disease. *Proteomics* **2003**, *3*, 1486–1494.
(27) Janowski, R.; Kozak, M.; Jankowska, E.; Grzonka, Z.; Grubb, A. Human cystatin C, an amyloidogenic protein, dimerizes through three-dimensional domain swapping. *Nat. Struct. Biol.* **2001**, *8*, 316–320.
(28) Mares, J.; Stejskal, D.; Vavrouskova, J.; Urbanek, K.; Herzig, R. Use of cystatin C determination in clinical diagnostics. *Biomed. Pap. Med. Fac. Univ. Palacky Olomouc Czech. Repub.* **2003**, *147*, 177–180.
(29) Jaskolski, M. 3D domain swapping, protein oligomerization, and amyloid formation. *Acta Biochim. Pol.* **2001**, *48*, 807–827.
(30) Serpell, L. C.; Blake, C. C.; Fraser, P. E. Molecular structure of a fibrillar Alzheimer's A beta fragment. *Biochemistry* **2000**, *39*, 13269–13275.
(31) Tycko, R. Insights into the amyloid folding problem from solid-state NMR. *Biochemistry* **2003**, *42*, 3151–3159.
(32) Petkova, A. T.; Ishii, Y.; Balbach, J. J.; Antzutkin, O. N.; Leapman, R. D. A structural model for Alzheimer's beta-amyloid fibrils based on experimental constraints from solid state NMR. *Proc. Natl. Acad. Sci. U.S.A.* **2002**, *99*, 16742–16747.

(33) Pike, C. J.; Walencewicz-Wasserman, A. J.; Kosmoski, J.; Cribbs, D. H.; Glabe, C. G. Structure−activity analyses of beta-amyloid peptides: contributions of the beta 25−35 region to aggregation and neurotoxicity. *J. Neurochem.* **1995**, *64*, 253–265.

(34) Miravalle, L.; Tokuda, T.; Chiarle, R.; Giaccone, G.; Bugiani, O. Substitutions at codon 22 of Alzheimer's abeta peptide induce diverse conformational changes and apoptotic effects in human cerebral endothelial cells. *J. Biol. Chem.* **2000**, *275*, 27110–27116.

(35) Ghiso, J.; Frangione, B. Amyloidosis and Alzheimer's disease. *Adv. Drug Delivery Rev.* **2002**, *54*, 1539–1551.

(36) Esler, W. P.; Stimson, E. R.; Ghilardi, J. R.; Lu, Y. A.; Felix, A. M. Point substitution in the central hydrophobic cluster of a human beta-amyloid congener disrupts peptide folding and abolishes plaque competence. *Biochemistry* **1996**, *35*, 13914–13921.

(37) Wahlbom, M.; Wang, X.; Lindstrom, V.; Carlemalm, E.; Jaskolski, M. Fibrillogenic oligomers of human cystatin C are formed by propagated domain swapping. *J. Biol. Chem.* **2007**, *282*, 18318−18326.

(38) Levy, E. Cystatin C: a potential target for Alzheimer's treatment. *Expert Rev. Neurother.* **2008**, *8*, 687–689.

(39) Dalboge, H.; Jensen, E. B.; Tottrup, H.; Grubb, A.; Abrahamson, M. High-level expression of active human cystatin C in *Escherichia coli*. *Gene* **1989**, *79*, 325–332.

(40) Damoc, E.; Youhnovski, N.; Crettaz, D.; Tissot, J. D.; Przybylski, M. High resolution proteome analysis of cryoglobulins using Fourier transform-ion cyclotron resonance mass spectrometry. *Proteomics* **2003**, *3*, 1425–1433.

(41) Comeau, S. R.; Gatchell, D. W.; Vajda, S.; Camacho, C. J. ClusPro: a fully automated algorithm for protein−protein docking. *Nucleic Acids Res.* **2004**, *32*, W96–W99.

(42) Tovchigrechko, A.; Vakser, I. A. GRAMM-X public Web server for protein−protein docking. *Nucleic Acids Res.* **2006**, *34*, W310–W314.

(43) Koradi, R.; Billeter, M.; Wuthrich, K. MOLMOL: a program for display and analysis of macromolecular structures. *J. Mol. Graphics* **1996**, *14*, 51–55, 29−32.

JM801115E